TASK-DEPENDENT MOVEMENT VARIABILITY IN GAIT CONTROL: A COMPUTATIONAL ACCOUNT

MATHILDE SIJTSMA

Abstract

When we walk, there are slight movement variations at every step due to the redundancy in the motor system; there are more degrees of freedom available in the lower extremities than necessary to control the feet. The uncontrolled manifold (UCM) framework can be used to dissociate task relevant and irrelevant variability of the joints stabilising the feet during walking. If there is more variability in the task irrelevant than relevant dimension, there is a synergy in the system. The optimal feedback control (OFC) framework focuses on variability control, suggesting that efficient motor control only corrects an ongoing movement if it deviates from the desired goal, as evident from changes in feedback gains and endpoint variability. Here we investigated whether both models provide a unifying explanation of task-dependent variability throughout the swing phase of gait – focusing on mediolateral ankle movements. Participants walked on narrow or wide targets projected on a treadmill, which were sometimes visually perturbed in the mediolateral direction. Consistent with our predictions, the synergy increased while endpoint variability decreased when participants stepped on narrow compared to wide unperturbed targets. In response to the perturbation of narrow targets, we observed increased feedback gains and decreased endpoint variability, which is consistent with the OFC account. However, the UCM model's synergy did not increase; instead, the organisation of variance in task relevant and irrelevant dimensions changed, resulting in an absence of a synergy in the final swing phase. Taken together, these results suggest that similar variability control of ankle movements can have different underlying variability organisations of the lower extremity joints. Our computational approach and experimental findings contribute to forming naturalistic sensorimotor models of task-dependent movement variability in healthy gait, which could also be used to enrich our understanding of neurologically impaired gait and its rehabilitation.

Keywords: Gait control, Uncontrolled Manifold Framework, Optimum Feedback Control

Supervisors
Prof. dr. Pieter Medendorp
Prof. dr. Noël Keijsers

Affiliation
Radboud University, Nijmegen, The Netherlands
Donders Centre for Cognition, Nijmegen, The Netherlands

Author contact
mathilde.sijstma@donders.ru.nl

Introduction

No motor task can exactly be repeated; there will always be slight variations between movements. For instance, we introduce variations in our cyclic arm strokes whilst swimming front crawl. This variability is possible due to the kinematic redundancy in the motor system, meaning that there are more degrees of freedom available than needed to perform a motor task (Bernstein, 1967). Variability in arm movements has often been investigated (e.g., Domkin et al., 2002; Keyser et al., 2017; Liu & Todorov, 2007; Romero et al., 2015). However, much less is known about our most frequently executed cyclic movement, walking. Two prominent sensorimotor theories that focus on understanding movement variations are the uncontrolled manifold (UCM; Scholz & Schöner, 1999) and optimal feedback control (OFC; Todorov & Jordan, 2002b). While the UCM model focuses on variability structure and the OFC model is directed at variability control, both make related predictions about variability along task relevant and irrelevant dimensions in a redundant motor system. Specifically, they both imply that some movement variability is left uncontrolled by the brain. Here, we investigate the performance of both models in explaining behaviour in the same gait task to examine whether their outcome variables complement each other. Moreover, it can help us to better understand the regulation of variability during gait.

The UCM model supports the notion that the brain could functionally organise the degrees of freedom within the motor system such that a particular performance variable is stabilised (Scholz & Schöner, 1999). In this model, all elemental variables (or degrees of freedom) that contribute to the performance variable span a state space, which is divided into two subspaces (Krishnan et al., 2013). One subspace is aligned with the manifold, consisting of all elemental variable configurations that do not influence the performance variable and can be left uncontrolled by the brain (i.e., the UCM). The other subspace, orthogonal to the manifold, contains the variance that affects task performance. If there is relatively more variance aligned with the manifold than orthogonal, the performance variable is stabilised and there is a synergy in the motor system. In other words, there is more variability left uncontrolled by the brain than there is variability requiring neural control. UCM analyses have been applied to sit-to-stand (Scholz & Schöner, 1999), force production (Friedman et al., 2009) and gait tasks (Devetak et al., 2022; Krishnan et al., 2013). These studies support that not all variability due to the redundancy in the motor system is suppressed, but instead is organised efficiently to optimise task performance.

While the UCM model accounts for the structure of variability, the OFC model makes predictions about how the brain controls the variability (Scott, 2004; Todorov & Jordan, 2002a, 2002b). One of the control principles of OFC is minimum intervention, meaning that people only correct for movement deviations following a perturbation if the deviation interferes with their task goal. This principle has frequently been investigated in arm reach studies where mechanical, visual or vestibular perturbations were introduced as participants reached to small (i.e., dot) or large (i.e., wide bar) targets (Keyser et al., 2017; Knill et al., 2011; Nashed et al., 2012). Movement traces were analysed to assess task-specific feedback gains, expressed as corrective movement adjustments after a perturbation. Generally, endpoint variability is lower while feedback gains are higher after perturbed reaches to small compared to large targets, reflecting the increased need for motor

control to maintain accurate task performance (Keyser et al., 2017; Knill et al., 2011; Nashed et al., 2012). In our everyday life, we constantly need to organise and control our motor system to adjust our gait to environmental demands. However, in neurological patients, such as stroke survivors, online corrections during gait are often biomechanically different or impaired (e.g., Arene & Hidler, 2009; Theunissen et al., 2020). To better understand the movement variability observed in impaired gait and to inform sensorimotor rehabilitation, we should invest in unraveling the mechanisms of healthy gait control. Specifically, the first aim of this study is to use the UCM and OFC frameworks to understand how variance is organised and controlled throughout the swing phase of gait in healthy individuals. Considering that both the UCM and OFC frameworks argue that some variability is left uncontrolled by the brain if it does not interfere with task performance, we examined whether there are similarities between the outcome variables of both models over the swing phase.

Movement variability in the swing phase of gait has previously been investigated using constraint-based walking tasks. Such studies found that a higher need for precision during walking, for instance when walking over a beam versus free overground walking, led to extended variance along, or suppressed variance orthogonal to the manifold (Rosenblatt et al., 2014, 2015; Shafizadeh et al., 2019). A commonly used constraint-based walking task is a precision stepping (e.g., Bank et al., 2011; Mazaheri et al., 2014). In one operation of this task, targets are projected onto a treadmill belt, and participants are instructed to step onto the targets. We encounter similar situations in our everyday life, for instance when we control our motor system to avoid stepping into a puddle of water on the pavement. However, the structure of variability during precision stepping has not been investigated before using the UCM analysis. Moreover, precision stepping towards small and large perturbed targets mimics the design of OFC studies in the arm reach literature but has not been investigated in the gait (e.g., Keyser et al., 2017; Knill et al., 2011; Nashed et al., 2012).
In the current study, we investigated variability during the swing phase in gait using a precision stepping task, focusing on mediolateral (frontal plane) ankle movements only. Healthy participants walked onto narrow (i.e., narrow condition) or wide (i.e., wide condition) targets projected on a treadmill. The narrow condition required higher precision compared to the wide condition. Therefore, we expected lower endpoint variability and a higher synergy in the narrow compared to wide condition (Keyser et al., 2017; Knill et al., 2011; Nashed et al., 2012; Rosenblatt et al., 2015).

We also tested the participants in conditions in which some targets were visually perturbed by a small mediolateral displacement at different timepoints during the swing phase. This required participants to adjust their swing foot trajectory to successfully reach perturbed narrow targets, while no trajectory adjustments were necessary for swings to the perturbed wide targets. Hence, the need for control only increased between unperturbed and perturbed swings to narrow targets (Keyser et al., 2017; Knill et al., 2011; Nashed et al., 2012; Rosenblatt et al., 2014), in particular for the later perturbations for which less correction time is available (Liu & Todorov, 2007). We expected that the synergy and the feedback gains would be higher, while endpoint variability would be lower, during perturbed swings that require a higher need for control.

Methods

Participants

We included eight healthy individuals (M age = 27 years; SD = 3) in the study who were able to walk for 60 minutes without assistive devices, and who did not have orthopaedic or neurological disorders, or injuries that likely affect gait. The medical ethics review committee of Arnhem and Nijmegen (case number 2023-16422) reviewed the study, and determined it is exempted from the Medical Research Involving Human Subjects Act (Wet Medisch-wetenschappelijk Onderzoek; WMO). The participants provided written informed consent prior to participating in the experiment.

Experimental Setup

All measurements were performed in the Gait Real-time Interactive Lab (GRAIL) of the Sint Maartenskliniek (GRAIL, Motek Medical BV, the Netherlands) (see Figure 1). The GRAIL includes an instrumented treadmill with a large semi-cylindrical screen in front and a VICON motion capture system with ten infrared cameras (VICON, Oxford, United Kingdom) that recorded the positions of 25 reflective markers (14 mm in diameter), placed at anatomical landmarks according to an adjusted version of the Plug-in Gait lower and upper body model (see Appendix A). Marker positions were sampled at 100 Hz. Additionally, markers were placed at the medial epicondyles of the femur and the medial malleolus of the tibia for calibration of the knee and ankle axes and anatomical planes. These calibration makers were removed prior to data collection. Before marker attachment, leg length and pelvis, knee and ankle width were manually measured, as well as full body length and weight.

The participants walked on the treadmill of the GRAIL during five conditions: 1) regular walking (i.e., regular condition), 2) precision stepping to wide targets (i.e., wide condition), 3) precision stepping to wide targets with perturbations (i.e., wide jumping condition), 4) precision stepping to narrow targets (i.e., narrow condition) and 5) precision stepping to narrow targets with perturbations (i.e., narrow jumping condition). The width of the narrow targets matched the width of the participant's shoes (M = 10.5 cm; SD = 0.7) with an additional 4 cm to provide visual feedback on foot placement accuracy (see Figure 2). The wide targets were four times the participant's shoe width, also with an additional 4 cm. All targets had the same length (i.e., the length of the participant's shoe [M = 27.8 cm; SD = 1.6] with an additional 4 cm for visual feedback). The targets were aligned with the participant's natural step time, stride length and step width, as determined during a baseline phase prior to the start of the experiment.

A perturbation consisted of a medial or lateral displacement of the target by the width of the participant's shoe (see Figure 3). Thus, the size of the perturbations (i.e., mediolateral displacements) was identical during the wide and narrow jumping condition. The perturbations of interest were in the lateral direction and presented to the left foot. They were introduced 0, 90 or 180 ms after heel strike of the opposite foot preceding the perturbation, with an additional

presentation delay of 40 – 70 ms due to the technical constraints of the real-time GRAIL system. Pilot data demonstrated that the three perturbation timings corresponded to target displacements during early, mid, or late swing. Approximately 25% of the perturbations were in medial direction or presented to the right foot to decrease the predictability of the perturbations.

All treadmill walking was performed at 1.2 m/s, which is regarded a comfortable walking speed for healthy individuals (Bohannon & Williams Andrews, 2011; Rosenblatt et al., 2015). The participants were secured in a safety harness which was attached to the ceiling to prevent falls in case they lost their balance. The screen in front of the treadmill was not used.

Figure 1: The GRAIL

Note. The setup consists of an instrumented treadmill on which targets were projected, a Vicon motion capture system and a safety harness.

Experimental Paradigm

Before testing the experimental conditions, there was a familiarisation phase to ensure the participants felt comfortable walking on the treadmill, and to collect baseline gait measurements of the step time (M = 0.5 s; SD = 0.03), stride length (M = 135.5 cm; SD = 8.3), and step width (M = 14.9 cm; SD = 3.3). The participants were instructed to walk in the middle of the treadmill relative to its anterior-posterior axis (i.e., the long side of the treadmill; sagittal plane), which was indicated with tape on the railing of the treadmill. After participants indicated they felt comfortable walking on the treadmill, the regular condition commenced, in which the participants walked freely on the treadmill for two minutes.

After a short stop of the treadmill, the participants started with the precision stepping conditions in a fixed order. The treadmill stopped after each condition. The instruction in each condition was to step anywhere on the targets that were projected onto the treadmill belt. If the participants did not attempt to step on the targets for approximately three perturbations in a row, they received verbal feedback from the researchers to try to step on the targets.

All participants started with the wide condition as the first precision stepping condition. After a short familiarisation period of approximately 20 seconds, they walked for two minutes onto wide targets that were projected on the treadmill (see Figure 2). This was followed by the wide jumping condition (see Figure 3). A total of 250 perturbations were presented, corresponding to approximately 25 minutes of walking, which was divided into 10 blocks containing between 20 and 30 perturbations. Of the 250 perturbations, 153 perturbations were in the lateral direction and presented to the left foot, consisting of 51 early, mid and late perturbations each. The rest of the perturbations were in the medial direction or presented to the right foot. The treadmill did not stop between the blocks. Within each block, there were intertrial intervals between the perturbations of three to eight strides to ensure that the participants not only recovered stable gait, but also to create a constant hazard rate to decrease the predictability of the perturbation onset. Considering that medial perturbations evoked cross-steps, they were followed by an intertrial interval of minimally five strides to ensure participants recovered stable gait.

After an optional rest, the narrow condition began (see Figure 2). Participants stepped for two minutes onto narrow targets that were projected on the treadmill. This was followed by the narrow jumping condition (see Figure 3). The procedure for this condition was the same as for the wide jumping condition, except for the width of the targets. All participants performed the experiment in the order as outlined above.

Figure 2: Schematic Representation of the Precision Stepping Design of the Wide and Narrow conditions.

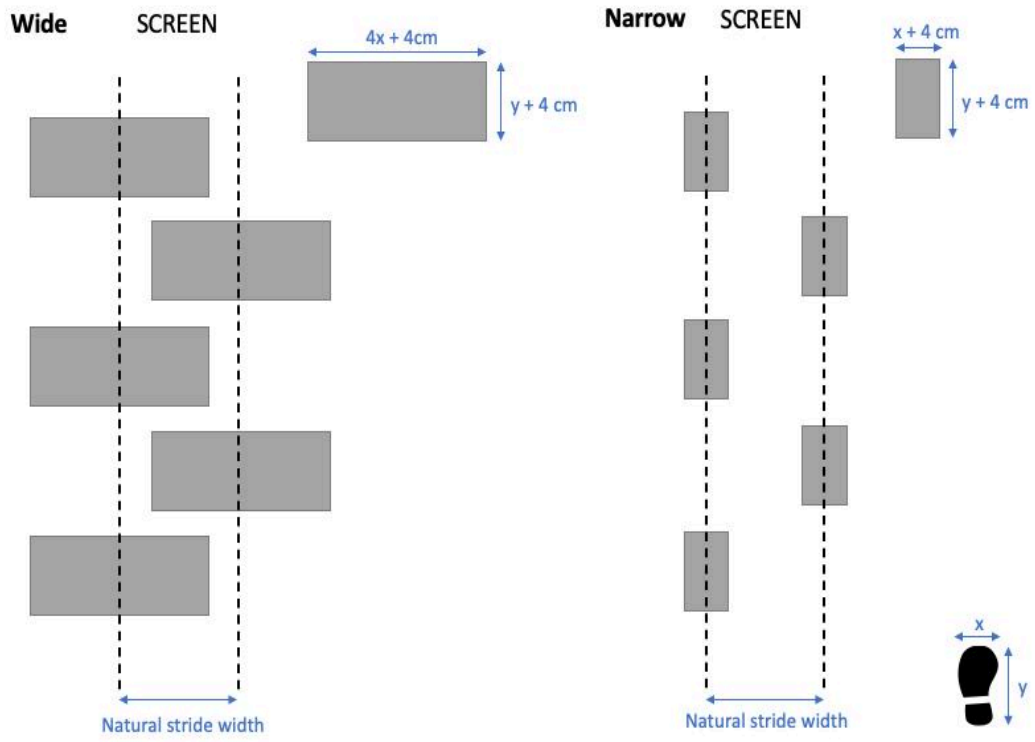

Figure 3: Schematic Representation of the Precision Stepping Design of the Wide and Narrow conditions.

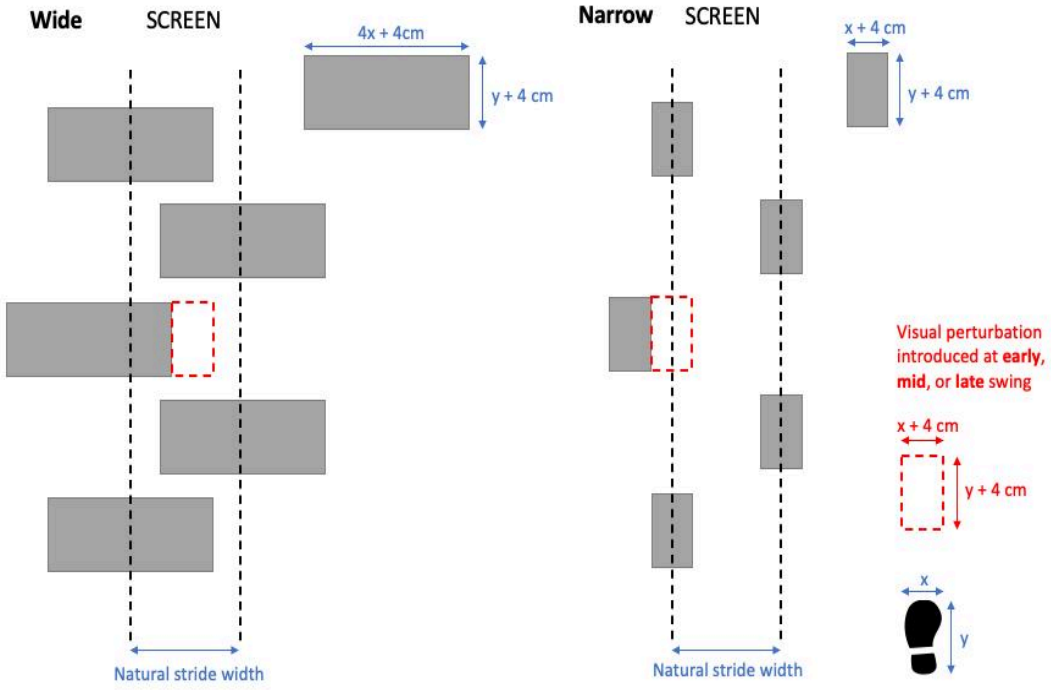

Note. The red rectangle with the dotted line represents the size of the mediolateral target displacement (i.e., the width of the participant's shoe with an additional 4 cm.

Data Analysis

The Process Dynamic Plug-in Gait Model pipeline operation was run on the marker position data in Vicon to obtain pelvis, knee and ankle joint centres. All position data were lowpass filtered with a zero lag, second-order Butterworth filter with a cut-off frequency of 10Hz (de Jong et al., 2020). Consistent with de Jong et al. (2020), toe off and heel strike events were determined using the position data of the foot markers. Toe off was defined as the instant where the toe marker (placed on the shoe at the level of the second metatarsal) started to move forwards (i.e., change from negative to positive velocity). Heel strike was defined as the instant where the heel marker (placed on the shoe at the level of the calcaneus) started to move backwards (i.e., change from positive to negative velocity).

Subsequently, the swings of the left leg from the regular, narrow and wide condition were extracted and analysed. For the narrow and wide jumping condition, only swings corresponding to the perturbations presented to the left foot in the lateral direction were extracted and analysed per perturbation timing. Of all these perturbed swings across all participants, three swings were unidentifiable from the motion tracking data and therefore excluded from the analyses.
Analyses were performed with MATLAB 2020b (The MathWorks Inc., 2020). Statistical tests on model outputs were conducted using R 4.2.2 (R Core Team, 2022) with R Studio (RStudio Team, 2021) and packages broom (Robinson et al., 2023), lsr (Navarro, 2015), rstatix (Kassambara, 2023b), tidyverse (Wickham et al., 2019) and ggpubr (Kassambara, 2023a).

Uncontrolled Manifold

The UCM analysis (Krishnan et al., 2013; Scholz & Schöner, 1999) was used to examine kinematic variability using a model linking angular displacements of lower-extremity joints (i.e., elemental variables) to the mediolateral ankle rajectory (i.e., performance variable) during the swing phase of gait. First, a geometric model was created, consisting of four segments : stance limb, 2) pelvis, 3) swing-limb thigh, and 4) swing-limb shank (see Figure 4). All $i \in \{1,2,3,4\}$ segments had a length Li. The pelvis segment had an angle θi relative to the horizontal in the frontal plane, while the other segments had an angle θi relative to the vertical in the frontal plane. The stance limb and swing-limb thigh segments had additionally motion in the sagittal plane, with angle α and γ, respectively. The pelvis segment had additional motion in the transverse plane, with angle β. We were only interested in the mediolateral ankle trajectory in the frontal plane. When the segments are projected on the frontal plane, their effective length changes, while they are constants in the geometric model. To account for these effective changes, the additional angles in the sagittal and transverse plane were included in the geometric model.

Figure 4: Geometric Model

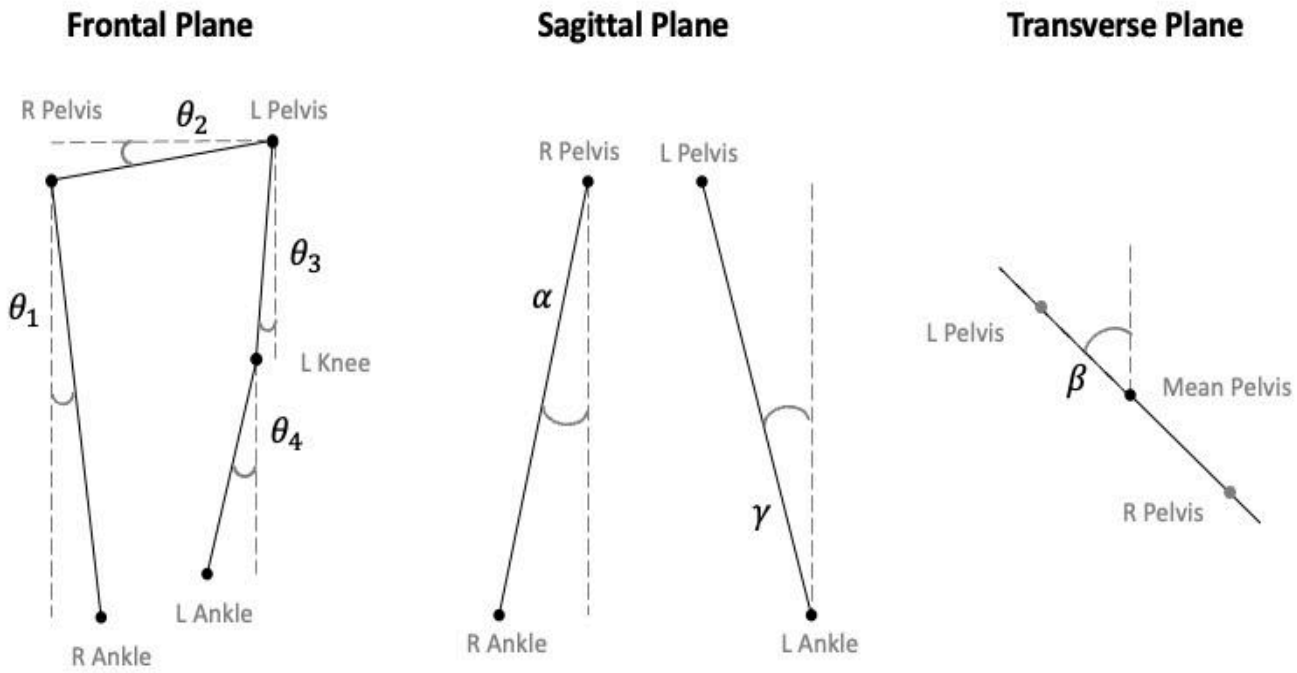

Note. For each joint, the joint centre was included in the geometric model. R = right; L = left.

The location of the ankle joint centre according to the geometric model was defined as:

$$\mathbf{AJC_{GM}} = L_1 \cos\alpha \sin\theta_1 + L_2 \cos\beta \cos\theta_2 + L_3 \cos\gamma \sin\theta_3 + L_4 \sin\theta_4$$

The corresponding elemental variables were defined as:

$$\Theta_{\mathbf{AJC_{GM}}} = [\theta_1 \quad \theta_2 \quad \theta_3 \quad \theta_4 \quad \alpha \quad \beta \quad \gamma]$$

By estimating $\mathbf{AJC_{GM}}$ and $\Theta_{\mathbf{AJC_{GM}}}$ at every sample of the motion tracking data, the trajectory of the ankle joint centre geometric model ($\Theta_{\mathbf{AJC_{GM}}}$) and the corresponding elemental variable matrix (Θ) were defined.

All further analyses were conducted separately for each participant and each condition (i.e., regular, narrow, wide, narrow jumping, and wide jumping) on the swings as outlined in the section "Data Analysis". Each swing phase contained a slightly different number of samples. Therefore, for all *N* swing phases, $\mathbf{AJC_{GM}}$ and Θ were interpolated from 1 to 100% (for every integer percentage). At every percentage of swing, the mean Θ was calculated across all swing phases ($\bar{\Theta}$).

We were interested in the organisation of variance, which is a linear concept, but the geometric model is non-linear. Therefore, we defined and evaluated the Jacobian around $\bar{\Theta}$ at every percentage of swing to obtain a linearised approximation of the forward kinematics. The Jacobian matrix contained the first-order partial derivatives of the trajectory coordinates with respect to the elemental variables. Hence, changes in joint angles and limb trajectory were linked through the Jacobian matrix.

$$\mathbf{J} = \left[\frac{\delta \mathbf{AJC_{GM}}}{\delta \Theta}\right]$$

$$= [L_1 \cos\alpha \cos\theta_1, -L_2 \cos\beta \sin\theta_2, L_3 \cos\gamma \cos\theta_3, L_4 \cos\theta_4, -L_1 \sin\alpha \sin\theta_1, -L_2 \sin\beta \cos\theta_2, -L_3 \sin\gamma \sin\theta_3]$$

The null space of the Jacobian represents the UCM, because it contains all combinations of Θ that do not affect the ankle joint trajectory. Hence, the brain does not have to control this variance. Thus, the null space was calculated so that $(\mathbf{J}(\bar{\Theta})) \cdot \boldsymbol{\varepsilon} = 0$ There are seven angles *n* = 7 and we were only interested in the mediolateral ankle trajectory *d* = 1 meaning that *n* − *d* = 6 basis vectors $\boldsymbol{\varepsilon}$ spanned the UCM at every percentage of swing.

$$\boldsymbol{\varepsilon} = null(\mathbf{J})$$

At every integer percentage of all *N* swings, we projected the deviations of the elemental variables from their mean ($\Theta - \bar{\Theta}$) onto a component aligned with the manifold, and a component orthogonal to the manifold:

$$\Theta_{\mathbf{UCM}} = \sum_{i=1}^{n-d} (\varepsilon_i^T \cdot (\Theta - \bar{\Theta}))^T \cdot \varepsilon_i$$

$$\Theta_{\mathbf{ORT}} = (\Theta - \bar{\Theta}) - \Theta_{\mathbf{UCM}}$$

The variance associated with both components, as well as the total variance in the elemental configuration space per degree of freedom, were calculated. The variance aligned with the manifold was normalised by *n* - *d* considering there are *n* - *d* basis vectors spanning the UCM. The variance orthogonal to the manifold was normalised by *d* because we only defined one subspace orthogonal to the manifold. This weighting of the variance aligned and orthogonal to the manifold was also incorporated in the total variance calculation.

$$V_{UCM} = \frac{1}{N}\frac{1}{n-d}\sum_{i=1}^{N}\Theta^2_{\mathbf{UCM}_i}$$

$$V_{ORT} = \frac{1}{N}\frac{1}{d}\sum_{i=1}^{N}\Theta^2_{\mathbf{ORT}_i}$$

$$V_{TOT} = \left(\tfrac{1}{n}\right)(dV_{ORT} + (n-d)V_{UCM})$$

The lower-extremity joints stabilise the mediolateral swing foot trajectory when $V_{UCM} > V_{ORT}$. Hence, the synergy index (ΔV) was calculated as the difference between the variance aligned with and orthogonal to the manifold, normalised by the total variance in the configuration space. Fisher's z-transformation was used to standardise the synergy index, with ΔV >= 0.390 representing the synergy.

$$\Delta V = \frac{V_{UCM} - V_{ORT}}{V_{TOT}} \qquad \Delta V_Z = \frac{1}{2}log\left[\frac{7+\Delta V}{(\frac{7}{6}-\Delta V)}\right]$$

The variance aligned with and orthogonal to the manifold, and the z-transformed synergy index were defined over swing from 1 to 100% as $\mathbf{V_{UCM}}, \mathbf{V_{ORT}}$ and $\Delta\mathbf{V_Z}$.

Statistical analysis. We calculated the mean $\mathbf{V_{UCM}}, \mathbf{V_{ORT}}$ and $\Delta\mathbf{V_Z}$ across participants per integer percentage of swing. In addition to inspecting of the visualisations of these variables, we also summarized $\Delta\mathbf{V_Z}$ by the mean and standard deviation for the beginning (1-33%), middle (33-66%) and final (67-100%) phase of swing. These means were compared using analyses of variance (ANOVAs). Thus, every statistical test was conducted separately per phase of swing.

The Shapiro-Wilk test and Mauchly's test indicated the ANOVA's assumptions of normality and sphericity were met, respectively. One-way repeated measures ANOVAs were conducted on the $^{\Delta\mathbf{V_Z}}$ to compare the unperturbed swings per condition (regular vs. wide vs. narrow). Additionally, one-way repeated measures ANOVAs were conducted on the $\Delta\mathbf{V_Z}$ to examine the effect of perturbation (unperturbed vs. early vs. mid vs. late), per target type (i.e.,wide or narrow). Furthermore, the effect of target (narrow vs. wide), perturbation timing (early vs. mid vs. late) and their interaction on $\Delta\mathbf{V_Z}$ was examined with repeated measures ANOVAs. We considered the results of the ANOVAs statistically significant at an alpha level of .05. If we found support for a significant interaction between the factors, we conducted post-hoc comparisons of their levels using False Discovery Rate (FDR) multiple comparisons hoc comparisons of their levels using False Discovery Rate (FDR) multiple comparisons correction. Where appropriate, statistical tests were evaluated against a two-tailed alternative hypothesis.

Optimal Feedback Control and the Minimum Intervention Principle

The OFC analysis was conducted separately for the movement position traces during swing, and their associated velocity traces. Each swing phase contained a slightly different number of samples, so the position and velocity traces were interpolated from 1 to 100%, for every integer percentage of swing. Consistent with the UCM analysis, we were only interested in the mediolateral movement direction of the ankle (i.e., frontal plane). We intended to compare endpoint variability and feedback gains of the unperturbed swings in the wide and narrow condition, and the perturbed swings in the wide and narrow jumping However, it is unwarranted to compare the perturbed swings of the wide and narrow jumping conditions if the unperturbed swings already differ from each other, which is an effect we expected based on the minimum intervention principle literature (e.g., Keyser et al.,2017; Knill et al., 2011; Nashed et al., 2012). Therefore, to assess the effect of the visual 2017; Knill et al., 2011; Nashed et al., 2012). Therefore, to assess the effect of the visual perturbations, for each perturbed swing we selected 10 unperturbed swings with the most similar initial (1-20%) mediolateral trajectory. For instance, for a perturbed swing of the narrow jumping condition, we selected the 10 most similar swings from the narrow condition. We chose the initial t = 1 - 20% of swing because we assume participants do not make corrective movements yet in this initial phase. The similarity between the perturbed and unperturbed swings was assessed using the reciprocal of the root mean squared (RMS) error (Keyser et al., 2017). A lower RMS error indicated higher similarity between the swings. The average of the 10 unperturbed swings per integer percentage of swing were subtracted from the perturbed swing of interest. Hence, the perturbed position and velocity traces were relative to the unperturbed traces, henceforward referred to as relative position and velocity traces. All further OFC results about perturbed swings pertain to the relative position and velocity traces.

Statistical analysis. Based on the position traces, we calculated the endpoint variability (i.e., standard deviation calculated at 100% over all swings) per participant, which was averaged to obtain the mean endpoint variability for the swings across participants. The mean endpoints of the unperturbed swings of the narrow versus wide targets were compared using a paired t-test. For the perturbed swings, a repeated measures ANOVA on mean endpoints was conducted to examine the effect of target (narrow vs. wide), perturbation timing (early vs. mid vs. late) and their interaction.

Furthermore, we calculated the maximum velocity based on the mean velocity traces across participants. The maximum velocities of the unperturbed swings of the narrow versus wide targets were compared using a paired t-test. For the perturbed swings, a repeated measures ANOVA on the relative maximum velocities was conducted to examine the effect of target (narrow vs. wide), perturbation timing (early vs. mid vs. late) and their interaction. For all OFC analyses, we used the Shapiro-Wilk test to check the t-test's and ANOVA's assumption of normality, and Mauchly's test to check the ANOVA's assumption of sphericity. The assumptions were met, except for one statistical test, where the assumption of sphericity was violated. Therefore, the Greenhouse-Geisser correction was applied to this test, indicated by p[GG]. We considered the results of the ANOVAs and t-tests statistically significant at an alpha level of .05. If the ANOVAs indicated a significant interaction between the factors, we conducted post-hoc comparisons of their levels using FDR multiple comparisons correction. Were appropriate, the statistical tests were evaluated against a two-tailed alternative hypothesis.

Results

Uncontrolled Manifold Analysis

Using our precision stepping paradigm and UCM framework, we aimed to examine whether the variance organisation changes and the synergy increases if the need for precision increases. We assumed the need for precision increases when walking on the narrow compared to the wide targets, and when the perturbations were introduced later compared to earlier during swing.

Effect of target during unperturbed swings

We compared the UCM variables corresponding to the unperturbed swings from the regular, wide and narrow condition per phase of swing (i.e., beginning, middle and final phase). Visual inspection of Figure 5A (left panel) suggested no effect of condition on $\mathbf{V_{UCM}}$ .However, $\mathbf{V_{ORT}}$ seemed lower throughout swing for the narrow compared to the wide and regular condition (see Figure 5B, left panel). This resulted in a consistently higher $\mathbf{\Delta V_Z}$ for the narrow compared to the wide and regular condition throughout swing (see Figure 5C, left panel). Consistent with this visual observation, the difference in $\mathbf{\Delta V_Z}$ between target conditions (regular vs. wide vs. narrow) was statistically significant in the beginning phase $(F(2,14) = 8.41, p = .004, \eta_p^2 = 0.55)$ and middle phase of swing $(F(2,14) = 8.02, p = .005, \eta_p^2 = 0.53)$. Planned comparisons demonstrated that swings to narrow targets resulted in a higher $\mathbf{\Delta V_Z}$ compared to swings to wide targets in the beginning phase of swing $(t(7) = 4.68, p = .006, d = 1.69)$. Additionally, swings to the narrow targets resulted in a higher $\mathbf{\Delta V_Z}$ compared to swings to wide targets $(t(7) = 2.99, p = .030, d = 0.85)$ or swings in the regular condition $(t(7) = 4.08, p = .014, d = 0.96)$ in the middle phase of swing. Hence, both the visual inspection of the UCM outcome variables in Figure 5 and that statistical tests support that the synergy index is higher during unperturbed swings if need for precision is higher.

Figure 5: Mean UCM variables throughout the swing phase, across all participants.

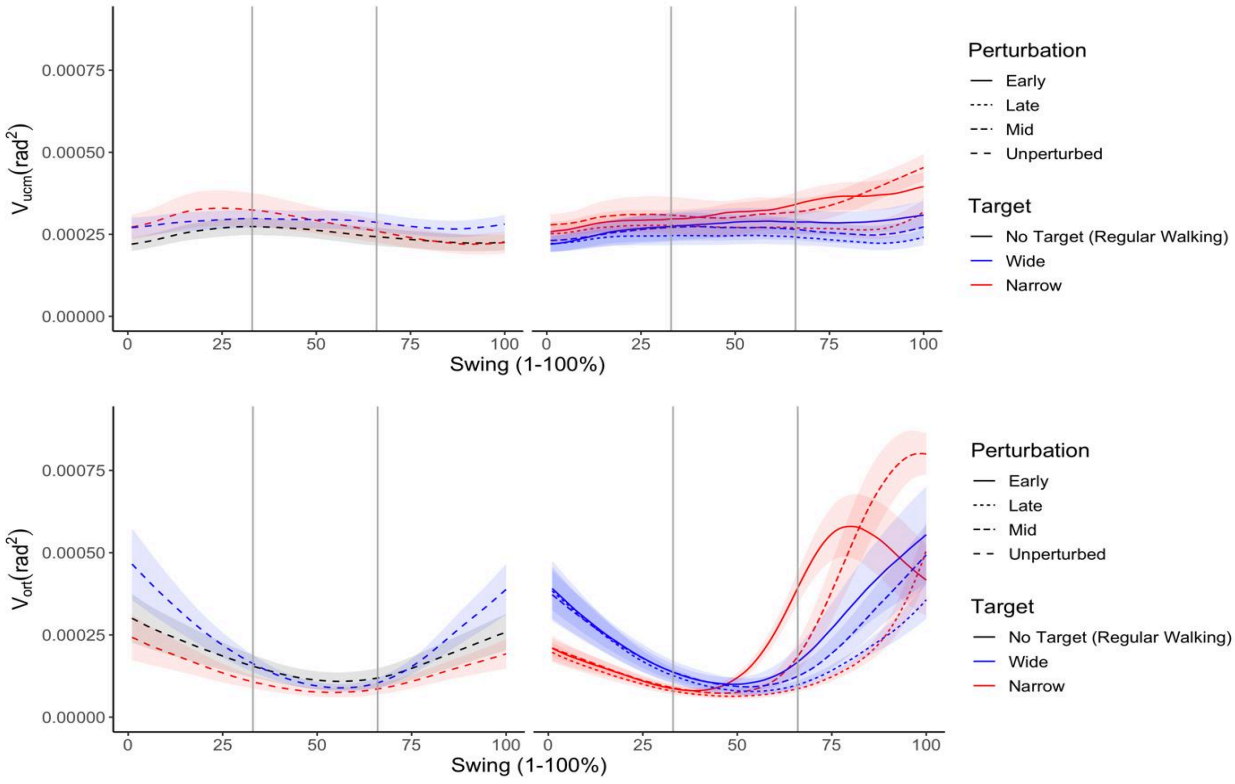

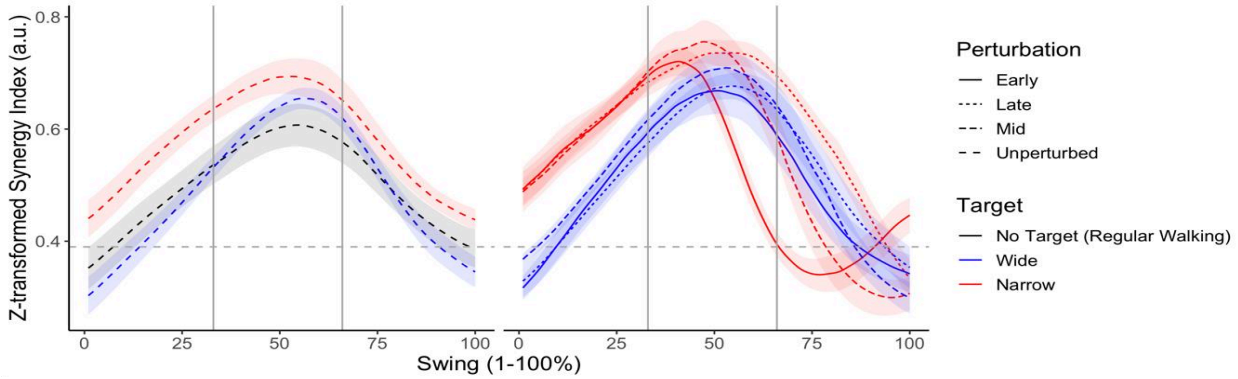

V_{UCM} (A), V_{ORT} (B) and ΔV_Z (C) for the unperturbed and perturbed swings per perturbation timing and target type, where applicable. The horizontal grey dashed line in panel C represents the minimum value (0.39) at which a synergy exists. The vertical grey lines demonstrate the beginning, middle and final phase of swing. Filled shading represents the standard error of the mean (SEM).

Effect of perturbation (i.e., unperturbed, early, mid and late)

We compared the UCM variables corresponding to the unperturbed, early perturbed, mid perturbed and late perturbed swings per phase of swing (i.e., beginning, middle and final phase). We repeated this analysis separately for the wide and narrow targets.

Wide targets

The V_{UCM} and V_{ORT} were similar for swings to unperturbed and perturbed wide targets (see Figure 5A; 5B). These variance organisations resulted in a similar ΔV_Z for the swings to unperturbed and perturbed wide targets in the beginning ($F(3,21) = 2.52$, $p = .086$), middle ($F(3,21) = 2.66$, $p = .074$) and final phase of swing ($F(3,21) = 0.60$, $p = .62$) (see Figure 5C). Hence, if the need for precision does not increase for the wide targets, then neither does the synergy index.

Narrow targets

Beginning phase. V_{UCM} and V_{ORT} were similar for swings to unperturbed and perturbed narrow targets in the beginning phase (see Figure 5A; 5B), resulting in a similar ΔV_Z ($F(3,21) = 2.15$, $p = 0.125$) (see Figure 5C). This suggests that the participants start their swing without adjustments in anticipation of a perturbation.

Middle phase. Compared to unperturbed narrow targets, V_{UCM} and V_{ORT} increased during the middle phase of the swings to perturbed narrow targets, particularly when the perturbation was presented early or mid swing (see Figure 5A; 5B). This resulted in a decrease in the ΔV_Z of the perturbed swings (see Figure 5C, right panel). This decrease occurred first for the early perturbed swings, followed by the mid and late perturbed swings. Hence, there seems to be a phase shift. The decrease in the ΔV_Z was less prominent for the unperturbed swings. Consistent with these observations, there was a significant effect of perturbation timing on ΔV_Z ($F(3,21) = 6.68, p = 0.002$, $\eta_p^2 = 0.49$). Specifically, the early perturbed swings had a lower ΔV_Z compared to the mid perturbed ($t(7) = 3.09$, $p = .018$, $d = 1.37$) and late perturbed swings ($t(7) = 4.91$, $p = 0.010$, $d = 1.89$).

Final phase. The trend observed during the middle phase of swing was continued in the late phase, with the $\mathbf{V}_{\mathbf{UCM}}$ and $\mathbf{V}_{\mathbf{UCM}}$ increasing for the perturbed swings, while this increase was less prominent in the unperturbed swings. Consequently, the $\Delta\mathbf{V}_{\mathbf{Z}}$ further decreased for the perturbed swings, and there was a significant effect of perturbation timing on $\Delta\mathbf{V}_{\mathbf{Z}} (F(3,21) = 8.03, p < .001, \eta_p^2 = 0.53)$ (see Figure 5C). The late perturbed swings had a higher $\Delta\mathbf{V}_{\mathbf{Z}}$ compared to early perturbed (t(7) = 3.14, p = .023, d = 1.84) and mid perturbed swings (t(7) = 6.18, p = .003, d = 1.48). Furthermore, the $\Delta\mathbf{V}_{\mathbf{Z}}$ was higher for the unperturbed swings than the early perturbed (t(7) = 1.86, p = .006, d = 2.07) and mid perturbed swings (t(7) = 2.80, p = .039, d = 1.63). These results are consistent with the graphs in Figure 5C, showing that the $\Delta\mathbf{V}_{\mathbf{Z}}$ of the perturbed swings decreases earlier than their unperturbed counterpart, with the early perturbed swings decreasing first, followed by the mid perturbed swings. Notably, the decrease in $\Delta\mathbf{V}_{\mathbf{Z}}$ for the early or mid perturbed swings to narrow targets led to an absence of a synergy in the late phase, while there was a synergy for the unperturbed counterpart.

Effect of target and perturbation

Finally, we examined the effect of target (narrow vs. wide) and perturbation timing (early vs. mid vs. late) together using a repeated measures ANOVA on $\Delta\mathbf{V}_{\mathbf{Z}}$, conducted per phase of swing.

Beginning phase. As expected from the parallel narrow and wide graphs in Figure 5C (right panel), there was a main effect of target in the beginning phase of swing $(F(1,7) = 29.23, p = .001, \eta_p^2 = 0.81)$, with the $\Delta\mathbf{V}_{\mathbf{Z}}$ of the swings to narrow targets being higher than swings to the wide targets (see Figure 5C, right panel). Similar to the aforementioned results of the unperturbed swings, this supports the prediction that the synergy index is higher if the need for precision is higher.

Middle phase. While the UCM variables corresponding to the wide targets did not change in response to the perturbations, the UCM variables corresponding to the narrow targets did change, especially in the middle phase of swing (see Figure 5C, right panel). Hence, there was an interaction between target and perturbation timing $(F(2,14) = 3.96, p = .043, \eta_p^2 = 0.361)$, suggesting that the effect of target type on $\Delta\mathbf{V}_{\mathbf{Z}}$ affected by perturbation timing. Additionally, there was a main effect of timing $(F(2,14) = 17.07, p < .001, \eta_p^2 = 0.71)$ of mid perturbed (t(7) = 5.28, p = .003, d = 1.87) and late perturbed swings (t(7)= 3.94, p = .008, d = 1.39) higher than the early perturbed swings. These effects could reflect the $\Delta\mathbf{V}_{\mathbf{Z}}$ decrease in the early perturbed swings to narrow targets that preceded the decrease in the mid and late perturbed swings.

Final phase. The $\Delta\mathbf{V}_{\mathbf{Z}}$ of all targets and timings decreased, but there appeared be a phase difference between the perturbation timings for the narrow targets (see Figure 5C, right panel). Hence, there was a main effect of timing $(F(2,14) = 6.29, p = .011, \eta_p^2 = 0.47)$, with the $\Delta\mathbf{V}_{\mathbf{Z}}$ of the late perturbed swings being higher than the early perturbed (t(7) = 3.07, p = .027, d = 1.09) and mid perturbed swings (t(7) = 3.10, p = .027, d = 1.10).

Optimal Feedback Control Analysis

Using our precision stepping paradigm and OFC framework, we aimed to examine whether endpoint variability decreases and feedback gains increase if the need for control increases, as predicted by the minimum intervention principle. We used the raw position traces (see Figure 6) and velocity traces for the comparisons between the unperturbed swings from the narrow and wide condition. We transformed these traces to relative estimates for the comparisons between the perturbed swings from the narrow and wide jumping condition.

Figure 6: Raw Position Traces of One Example Participant

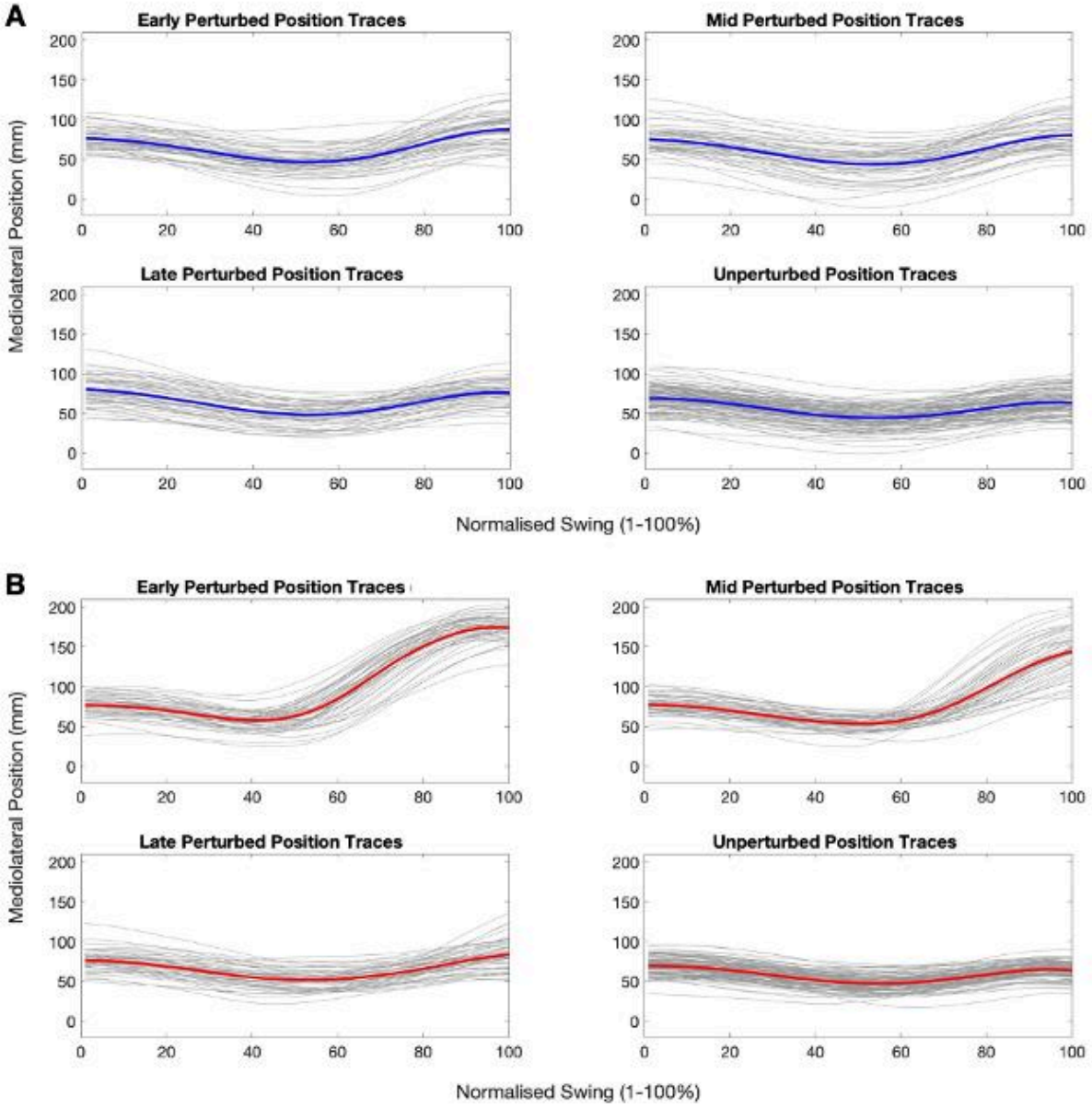

Note. A) Position traces of perturbed swings from the wide jumping condition, and unperturbed swings from the wide condition. B) Position traces of perturbed swings from the narrow jumping condition, and unperturbed swings from the narrow condition. All traces correspond to the left ankle. For each plot, the thick blue or red graph represents the mean position trace across swings.

Endpoint Variability

We compared the endpoint variability of the steps to unperturbed narrow and wide targets (see Figure 7A), and found that endpoint variability for the unperturbed swings to wide targets was significantly higher compared to the unperturbed swings to narrow targets ($t(7) = 5.41$, $p = .001$, $d = 1.91$). Additionally, for the perturbed swings, we examined the effect of target (narrow vs. wide) and perturbation timing (early vs. mid vs. late) together using a repeated measures ANOVA on relative endpoint variability (see Figure 7B). There was a main effect of target, with the relative endpoint variability larger for swings to wide compared to narrow targets

Hence, we found support for our prediction that endpoint variability is lower for the narrow targets – which require a higher need for control – compared to the wide targets. However, we did not observe an effect of perturbation timing (F(2,14) = 1.00, p = .392) or an interaction between target type and perturbation timing (F(1.06,7.43) = 2.00, p[GG] = .198).

Figure 7: Endpoint variablity

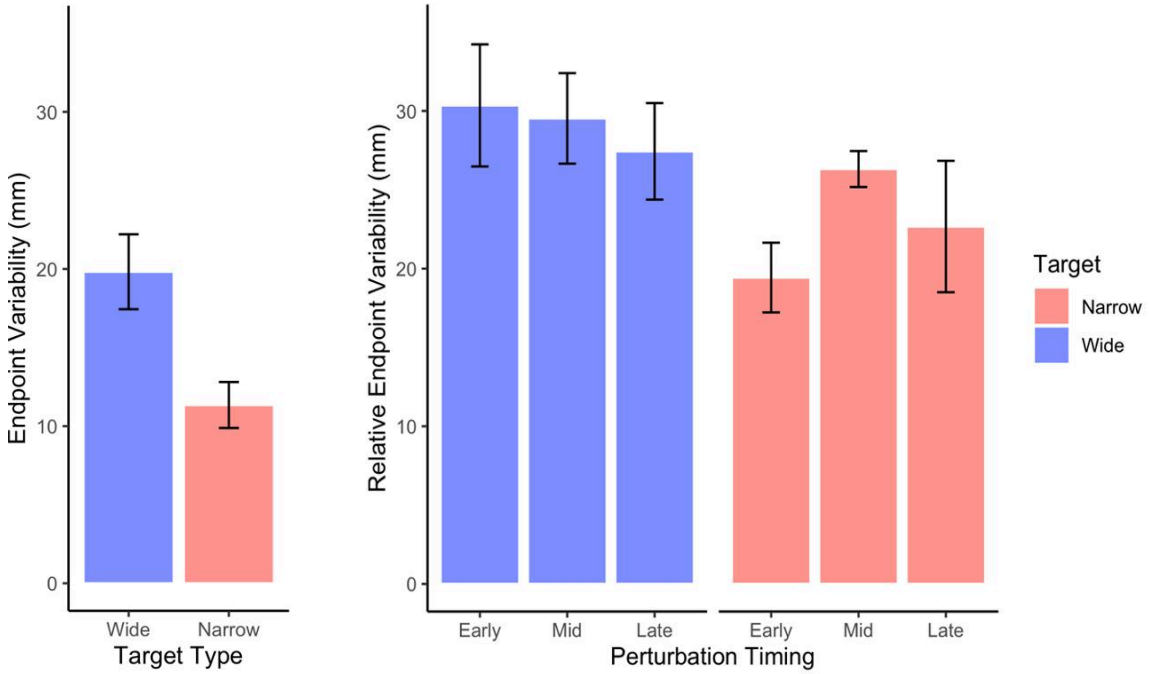

Note. A) Mean endpoint variability of the unperturbed swings in the wide and narrow condition, across all participants. B) Mean relative endpoint variability of the perturbed swings in the wide and narrow jumping condition, across all participants. Error bars represent the SEM.

Feedback gains

As mentioned previously, we operationalised the feedback gains as maximum lateral ankle velocity during swing. We found no support for a significant difference between the maximum velocity of the unperturbed narrow and wide swings (t(7) = 0.01, p = .993). Generally, based on visual inspection, there seemed to be no difference between the velocities of the swings to the unperturbed wide or narrow targets (see Figure 8A). Additionally, for the perturbed swings, we examined the effect of target (narrow vs. wide) and perturbation timing (early vs. mid vs. late) together using a repeated measures ANOVA on relative maximum velocity (see Figure 8B). There was a main effect of target, with maximum velocity being higher for swings to narrow compared to wide targets $(F(1,7) = 113.82, p < .001, \eta_p^2 = 0.94)$. We also observed a main effect of timing $(F(1,7) = 52.94, p < .001, \eta_p^2 = 0.88)$. The relative maximum velocity for the early perturbed swings was higher than for the mid perturbed (t(7) = 3.27, p = .014, d = 1.15) or late perturbed swings (t(7) = 10.6, p < .001, d = 3.76). Additionally, the relative maximum velocity was higher for the mid perturbed than for the late perturbed swings (t(7) = 7.19, p < .001, d = 2.54). Thus, in line with our predictions, the feedback gains were higher for swings to narrow compared to wide targets. Yet the earlier perturbations – and not the later ones – were associated with the highest feedback gains. We did not observe an interaction between target type and perturbation timing (F(2,14) = 3.68, p = .052).

For an overview of all statistical results, please see Appendix B.

Figure 8: Velocity Traces

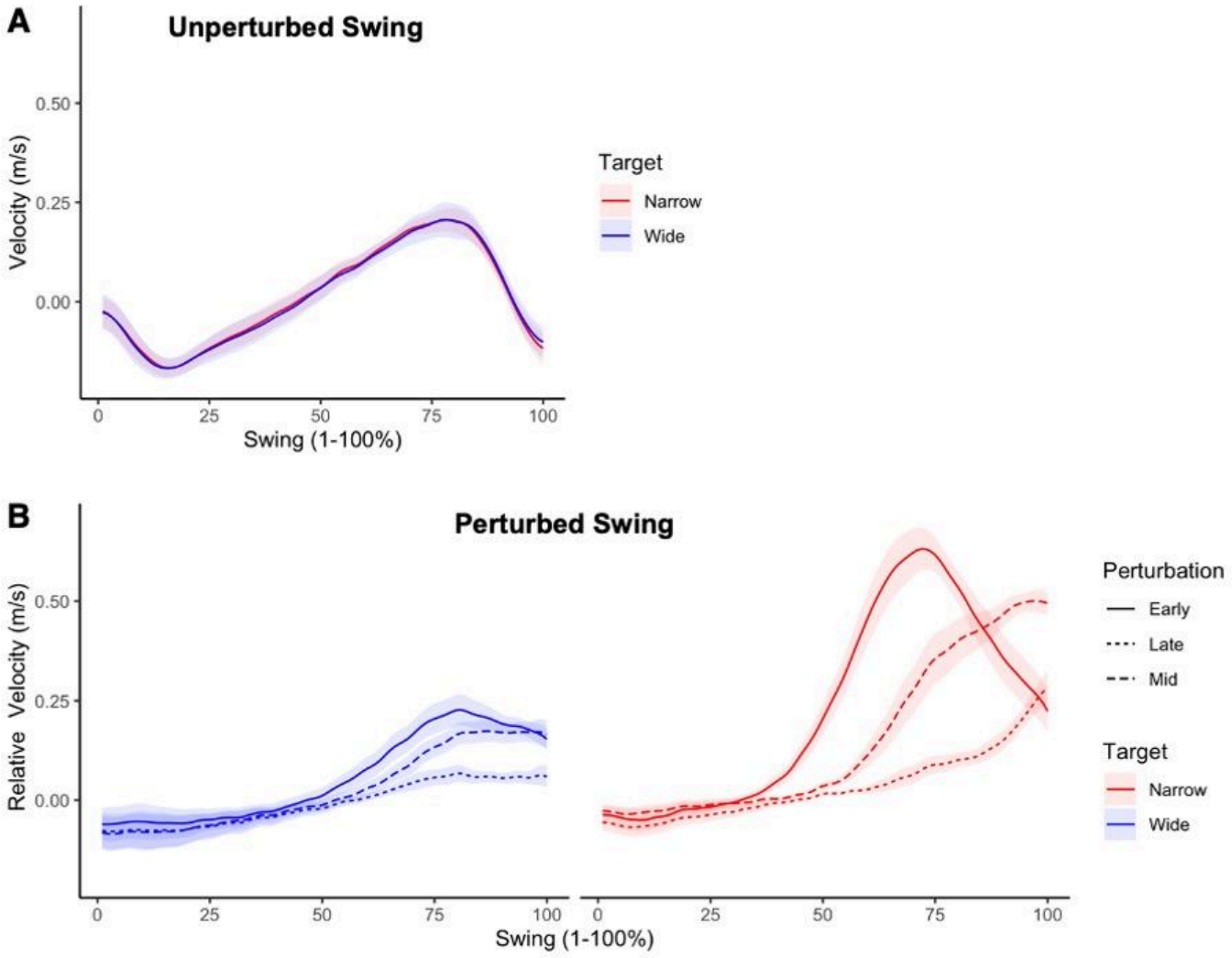

Note. A) Mean velocity traces of the unperturbed swings in the wide and narrow condition, across all participants. B) Mean relative velocity traces of the perturbed swings in the wide jumping and narrow jumping condition per perturbation timing, across all participants. Filled shading represents the SEM.

Discussion

Participants walked onto narrow or wide targets, which we visually perturbed to manipulate the level of precision and control required for the task. When participants stepped towards displaced narrow targets, they had to adjust their ankle trajectory to position their foot successfully into the target. This resulted in an increased need for control, particularly for perturbations later in the swing phase. In contrast, no trajectory adjustments were required for perturbed wide targets, so the need for control remained constant. We used this paradigm and the UCM framework to investigate the structure of the variability of the joints stabilising mediolateral ankle movements. Additionally, we investigated ankle endpoint variability and feedback gains with the OFC framework. We also examined whether the outcome variables of both models complemented each other. Generally, we expected that the synergy and feedback gains would increase, while endpoint variability would decrease, if need for control increased.

The findings related to the unperturbed walking conditions were in line with our predictions and consistent with the prior literature. The variance orthogonal to the manifold was lower – and so the synergy was higher – during the narrow condition compared to the regular or wide condition. Additionally, the ankle endpoint variability was lower during unperturbed swings to narrow compared to wide targets. These results are consistent with previous accounts of synergies during constrained walking (Rosenblatt et al., 2014, 2015) and endpoint variability during arm reaches (Keyser et al., 2017; Knill et al., 2011; Nashed et al., 2012). We found no differences in the feedback gains of the swings to unperturbed narrow or wide targets, which is also consistent with previous observations (e.g., Nashed et al., 2012). Altogether, we showed that 1) UCM findings observed during constrained walking were replicated during precision stepping, 2) the minimum intervention principles observed for unperturbed arm reaches were replicated in gait, and 3) the UCM and OFC outcome variables complemented each other for unperturbed swings.

For the perturbed swings, we did not find an increased synergy between swings to narrow compared to wide targets, but rather a change in the variance organisation. The interaction between target size and perturbation timing influenced the synergy index during the middle phase of swing. Both the wide and narrow perturbed swings exhibited peaks in this phase, with a seemingly higher peak for the narrow targets (see Figure 5C, right panel). However, this difference was not significant. For the perturbed swings to narrow targets, the peak was followed by a decline in the synergy index during the middle phase of swing. This pattern corresponded to the increase in orthogonal variance, which could reflect various phenomena. For instance, when a target was perturbed, there was a range of response times possible for initiating the movement correction, leading to increased variance. Furthermore, the mediolateral ankle movements made in the narrow jumping condition demand additional control beyond what is necessary for making anterior-posterior leg movements. Biological noise is signal-dependent, so this added control further contributes to the increased variance (e.g., Harris & Wolpert, 1998).

As a result of the increasing orthogonal variance, there was no synergy for the early and mid-perturbed swings to narrow targets in the final phase of swing; the seven degrees of freedom in the lower extremities could no longer stabilise the mediolateral ankle movement. Yet, there was a synergy for the late perturbed swings. Potentially, the need for precision remained high for the late perturbed swings, but the corrective movements were not fully executed due to the shorter time participants had to adjust their trajectory (see Figure 6B). In line with the aforementioned signal-dependent noise argument, the smaller movements resulted in less orthogonal variance, thereby preserving the synergy. In summary, the results of the jumping conditions suggest that perturbing swing does not per se lead to a higher synergy but could rather result in a different

variance structure compared to the unperturbed swings.

Our findings indicate that when faced with specific perturbations, healthy individuals seek compensation outside of the manifold instead of increasing the variance within the manifold to maintain the stability of the ankle trajectory. This could be an adaptive strategy for solving the motor task. Future studies could conduct the precision stepping task at various stages of the rehabilitation of stroke survivors to investigate whether they use a similar strategy to structure variance and solve the task, and whether this strategy is constant over time. Such investigations could provide valuable insights into potential indicators of stroke recovery beyond clinical observations.

Based on our OFC analysis of the perturbed swings, we observed an effect of target size but found no support for our predicted effect of perturbation timing. Consistent with the established literature on target size effects, the endpoint variability was lower while maximum velocity was higher for the narrow compared to wide perturbed swings (Keyser et al., 2017; Knill et al., 2011; Nashed et al., 2012). However, there was no support for our predicted effect of perturbation timing, which could be attributed to the time constraints of the swing phase. For instance, participants had more time to increase their velocity after an early perturbation, which could explain why the feedback gains were higher for the earlier compared to later perturbations. Furthermore, due to the time constraints, the later perturbations were most challenging, particularly for participants with a shorter step length and swing duration. Nevertheless, our pilot measurements and previous research (Zhang et al., 2020) indicated that correcting for the late perturbations was feasible. Because we included all left lateral perturbed swings in our analyses, we included some unsuccessful trials where the ankle trajectory was not corrected, and the number of unsuccessful trials might differ between participants. This might have inflated the variance on the mean endpoint variability – particularly for the more difficult late perturbations – and concealed perturbation timing effects. As a recommendation for future studies, we suggest to only select the swing phases where participants reached the target.

We have some additional points of consideration for follow-up investigations. Firstly, the participants could use different strategies to respond to the perturbations. As the targets were projected on the treadmill, participants could have rotated their foot to reach the target with their forefoot. This rotation strategy does not generate mediolateral displacements of the ankle joint, so the corrections are not included in our UCM or OFC models. Hence, particularly for the more challenging tasks, the ankle displacements could give the impression that the participants did not fully correct for a perturbation, while their forefoot was on the target. This might explain the smaller displacements in response to late perturbations shown in Figure 6B. Therefore, future studies could model mediolateral forefoot trajectories, instead of the ankle. Secondly, all participants walked at a fixed speed of 1.2 m/s. While this is regarded a comfortable walking speed, there are individual differences in preferred walking speed, stride length and stride time (Bohannon, 1997; Bohannon & Williams Andrews, 2011; Dingwell et al., 2010). Hence, the trials with later perturbations were easier for participants with a longer step time. Therefore, follow-up investigations could personalise the task per participant.

Thirdly, we did not counterbalance the conditions, because we anticipated that walking on the narrow (perturbed) targets would require more control than walking on the wide targets. As a result, we expected that exposure to the narrow conditions would influence performance in the wide conditions more than vice versa. Follow-up studies could counterbalance the conditions to investigate such effects further. Fourthly, we performed our statistical test on the synergy index per phase of swing, which could conceal true effects. We recommend future studies to analyse the synergy index per percentage of swing, for instance using clustering analyses or statistical parametric mapping (Pataky, 2010). Lastly, we operationalised the feedback gains as maximum velocity. Alternatively, future studies could operationalise the feedback gains as the slope of the velocity traces between 25 – 75% of the peak difference (Oostwoud Wijdenes et al., 2019). In other words, they could operationalise the gains in terms of acceleration, because changes in acceleration precede changes in velocity and would therefore be more precise estimates of the feedback gains.

Conclusion

We found that the outcomes of UCM and OFC analyses are complementary for the unperturbed swings, as the synergy increased, and the endpoint variability decreased for swings to the narrow targets that required a higher level of precision and control. The OFC analysis of the perturbed swings demonstrated that the feedback gains increased while endpoint variability decreased when participants walked on the narrow targets. However, we did not find a complementary increase in the UCM model's synergy; instead, participants structured their variance differently. As a result, they could not stabilise their mediolateral ankle trajectory anymore with the same degrees of freedom as used for the steps to unperturbed targets. These findings suggest that similar variability control of ankle movements can have different underlying variability organisations of the lower extremity joints. We hope our study contributes to forming naturalistic sensorimotor models of task-dependent movement variability in healthy gait, which could also be used to complement our understanding of neurologically impaired gait and its rehabilitation.

References

Arene, N., & Hidler, J. (2009). Understanding motor impairment in the paretic lower limb after a stroke: A review of the literature. Topics in Stroke Rehabilitation, 16(5), 346–356. https://doi.org/10.1310/tsr1605-346

Bank, P. J. M., Roerdink, M., & Peper, C. E. (2011). Comparing the efficacy of metronome beeps and stepping stones to adjust gait: Steps to follow! Experimental Brain Research, 209(2), 159–169. https://doi.org/10.1007/s00221-010-2531-9

Bernstein, N. A. (1967). The co-ordination and regulation of movements ([1st English ed.]). Pergamon Press.

Bohannon, R. W. (1997). Comfortable and maximum walking speed of adults aged 20—79 years: Reference values and determinants. Age and Ageing, 26(1), 15–19. https://doi.org/10.1093/ageing/26.1.15

Bohannon, R. W., & Williams Andrews, A. (2011). Normal walking speed: A descriptive meta-analysis. Physiotherapy, 97(3), 182–189. https://doi.org/10.1016/j.physio.2010.12.004

de Jong, L. A. F., van Dijsseldonk, R. B., Keijsers, N. L. W., & Groen, B. E. (2020). Test-retest reliability of stability outcome measures during treadmill walking in patients with balance problems and healthy controls. Gait & Posture, 76, 92–97. https://doi.org/10.1016/j.gaitpost.2019.10.033

Devetak, G. F., Rinaldin, C. D. P., Ranciaro, M., Neto, G. N. N., Bohrer, R. C. D., & Manffra, E. F. (2022). Does the number of steps needed for UCM gait analysis differs between healthy and stroke? Journal of Biomechanics, 144, 111353. https://doi.org/10.1016/j.jbiomech.2022.111353

Dingwell, J. B., John, J., & Cusumano, J. P. (2010). Do humans optimally exploit redundancy to control step variability in walking? PLOS Computational Biology, 6(7), e1000856. https://doi.org/10.1371/journal.pcbi.1000856

Domkin, D., Laczko, J., Jaric, S., Johansson, H., & Latash, M. (2002). Structure of joint variability in bimanual pointing tasks. Experimental Brain Research, 143, 11–23. https://doi.org/10.1007/s00221-001-0944-1

Friedman, J., Skm, V., Zatsiorsky, V. M., & Latash, M. L. (2009). The sources of two components of variance: An example of multifinger cyclic force production tasks at different frequencies. Experimental Brain Research, 196(2), 263–277. https://doi.org/10.1007/s00221-009-1846-x

Harris, C. M., & Wolpert, D. M. (1998). Signal-dependent noise determines motor planning. Nature, 394(6695), 780–784. https://doi.org/10.1038/29528

Kassambara, A. (2023a). ggpubr: 'ggplot2' Based Publication Ready Plots (0.6.0) [R]. https://CRAN.R-project.org/package=ggpubr

Kassambara, A. (2023b). rstatix: Pipe-friendly framework for basic statistical tests (0.7.2) [R]. https://CRAN.R-project.org/package=rstatix

Keyser, J., Medendorp, W. P., & Selen, L. P. J. (2017). Task-dependent vestibular feedback responses in reaching. Journal of Neurophysiology, 118(1), 84–92. https://doi.org/10.1152/jn.00112.2017

Knill, D. C., Bondada, A., & Chhabra, M. (2011). Flexible, task-dependent use of sensory feedback to control hand movements. The Journal of Neuroscience, 31(4), 1219–1237. https://doi.org/10.1523/JNEUROSCI.3522-09.2011

Krishnan, V., Rosenblatt, N. J., Latash, M. L., & Grabiner, M. D. (2013). The effects of age on stabilization of the mediolateral trajectory of the swing foot. Gait & Posture, 38(4), 923–928. https://doi.org/10.1016/j.gaitpost.2013.04.023

Liu, D., & Todorov, E. (2007). Evidence for the flexible sensorimotor strategies predicted by optimal feedback control. Journal of Neuroscience, 27(35), 9354–9368. https://doi.org/10.1523/JNEUROSCI.1110-06.2007

Mazaheri, M., Roerdink, M., Bood, R. J., Duysens, J., Beek, P. J., & Peper, C. (Lieke) E. (2014). Attentional costs of visually guided walking: Effects of age, executive function and stepping-task demands. Gait & Posture, 40(1), 182–186. https://doi.org/10.1016/j.gaitpost.2014.03.183

Nashed, J. Y., Crevecoeur, F., & Scott, S. H. (2012). Influence of the behavioral goal and environmental obstacles on rapid feedback responses. Journal of Neurophysiology, 108(4), 999–1009. https://doi.org/10.1152/jn.01089.2011

Navarro, D. J. (2015). Learning statistics with R: A tutorial for psychology students and other beginners. (0.5.1) [R]. University of New South Wales. https://learningstatisticswithr.com

Oostwoud Wijdenes, L., van Beers, R. J., & Medendorp, W. P. (2019). Vestibular modulation of visuomotor feedback gains in reaching. Journal of Neurophysiology, 122(3), 947–957. https://doi.org/10.1152/jn.00616.2018

Pataky, T. C. (2010). Generalized n-dimensional biomechanical field analysis using statistical parametric mapping. Journal of Biomechanics, 43(10), 1976–1982. https://doi.org/10.1016/j.jbiomech.2010.03.008

R Core Team. (2022). R: A language and environment for statistical computing (4.2.2) [Computer software]. R Foundation for Statistical Computing. https://www.R-project.org/

Robinson, D., Hayes, A., & Couch, C. (2023). broom: Convert statistical objects into tidy tibbles (R package version 1.0.3) [Computer software]. https://CRAN.R-project.org/package=broom

Romero, V., Kallen, R., Riley, M., & Richardson, M. (2015). Can joint action be synergistic? Studying the stabilization of interpersonal hand coordination. Journal of Experimental Psychology. Human Perception and Performance, 41(5), 1223–1235.

Rosenblatt, N. J., Hurt, C. P., Latash, M. L., & Grabiner, M. D. (2014). An apparent contradiction: Increasing variability to achieve greater precision? Experimental Brain Research, 232(2), 403–413. https://doi.org/10.1007/s00221-013-3748-1

Rosenblatt, N. J., Latash, M. L., Hurt, C. P., & Grabiner, M. D. (2015). Challenging gait leads to stronger lower-limb kinematic synergies: The effects of walking within a more narrow pathway. Neuroscience Letters, 600, 110–114. https://doi.org/10.1016/j.neulet.2015.05.039

RStudio Team. (2021). RStudio: Integrated development environment for R [Computer software]. RStudio, PBC. http://www.rstudio.com/

Scholz, J. P., & Schöner, G. (1999). The uncontrolled manifold concept: Identifying control variables for a functional task. Experimental Brain Research, 126(3), 289–306. https://doi.org/10.1007/s002210050738

Scott, S. H. (2004). Optimal feedback control and the neural basis of volitional motor control. Nature Reviews Neuroscience, 5(7), 532–545. https://doi.org/10.1038/nrn1427

Shafizadeh, M., Wheat, J., Kelley, J., & Nourian, R. (2019). Stroke survivors exhibit stronger lower extremity synergies in more challenging walking conditions. Experimental Brain Research, 237(8), 1919–1930. https://doi.org/10.1007/s00221-019-05560-9

The MathWorks Inc. (2020). MATLAB Version: 9.9.0.1718557 (R2020b) (9.9.0.1718557) [Computer software]. The MathWorks Inc. https://www.mathworks.com

Theunissen, T., Ensink, C., Bakker, R., & Keijsers, N. (2020). Movin(g) reality: Rehabilitation after a CVA with augmented reality. Proceedings of the European Conference on Pattern Languages of Programs 2020, 1–7. https://doi.org/10.1145/3424771.3424819

Todorov, E., & Jordan, M. I. (2002b). Optimal feedback control as a theory of motor coordination. Nature Neuroscience, 5(11), 1226–1235. https://doi.org/10.1038/nn963

Vicon Motion Systems. (2021). Plug-in Gait reference guide. https://docs.vicon.com/display/Nexus212/Plug-in+Gait+Reference+Guide

Wickham, H., Averick, M., Bryan, J., Chang, W., McGowan, L. D., François, R., Grolemund, G., Hayes, A., Henry, L., Hester, J., Kuhn, M., Pedersen, T. L., Miller, E., Bache, S. M., Müller, K., Ooms, J., Robinson, D., Seidel, D. P., Spinu, V., … Yutani, H. (2019). Welcome to the Tidyverse. Journal of Open Source Software, 4(43), 1686. https://doi.org/10.21105/joss.01686

Zhang, Y., Smeets, J. B. J., Brenner, E., Verschueren, S., & Duysens, J. (2020). Fast responses to stepping-target displacements when walking. The Journal of Physiology, 598(10), 1987–2000. https://doi.org/10.1113/JP278986

Appendix A

Marker Positions

Table A1. Marker positions according to an adjusted version of the Plug-in Gait lower and upper body model.

Segment	Marker	Anatomical position
Torso	C7 marker	Spinous process of 7th cervical vertebra
Shoulder	Shoulder marker	Acromioclavicular joints
Upper arm	Elbow marker	Lateral epicondyles of the humerus
Forearm	Wrist marker	Most lateral aspect of the ulna
Pelvis (ASI)	Anterior pelvis marker	Anterior superior iliac splines
Pelvis (PSI)	Posterior pelvis marker	Posterior superior iliac splines
Thigh	Thigh marker	Lateral thigh: Half distance between the trochanter major and lateral epicondyle of the femur
Thigh	Knee marker	Lateral epicondyles of the femur
Thigh	Knee marker – *only for calibration*	Medial epicondyles of the femur
Shank	Tibia marker	Lateral shank: Half distance between lateral epicondyle of the femur and lateral malleolus of the fibula
Shank	Ankle marker	Lateral malleolus of the fibula
Shank	Ankle marker – *only for calibration*	Medial malleolus of the tibia
Foot	Toe marker	Head of second metatarsal *Note.* Marker placed on the shoe
Foot	Heel marker	Posterior aspect of calcaneus inferior, at the same height with respect to plantar surface of the foot as the toe marker *Note.* Marker placed on the shoe
Foot	Shoe edge marker	Most anterior aspect of the shoe *Note.* Marker placed on the shoe

Note. Adapted from the Plug-in Gait Reference Guide (Vicon Motion Systems, 2021)

Appendix B

Statistical Results

Table B1: Results of Statistical Tests

Analysis	Dependent Variable	Factor(s) with Levels	Statistic	*p*	Effect size
UCM Unperturbed	ΔV_Z beginning	Target condition (regular vs. wide vs. narrow)	$F(2,14) = 8.48$	.004	0.55
		Post-hoc: narrow > wide	$t(7) = 4.69$	.007	1.69
	ΔV_Z middle	Target condition (regular vs. wide vs. narrow)	$F(2,14) = 8.02$	.005	0.53
		Post-hoc: narrow > regular	$t(7) = 4.08$	.014	0.96
		Post-hoc: narrow > wide	$t(7) = 2.99$	.030	0.85
	ΔV_Z final	Target condition (regular vs. wide vs. narrow)	$F(2,14) = 3.09$	.078	
UCM Narrow Targets	ΔV_Z beginning	Perturbation timing (unperturbed vs. early vs. mid vs. late)	$F(3,21) = 2.15$	.125	
	ΔV_Z middle	Perturbation timing (unperturbed vs. early vs. mid vs. late)	$F(3,21) = 6.68$	.002	0.49
		Post-hoc: mid > early	$t(7) = 3.90$	.018	1.37
		Post-hoc: late > early	$t(7) = 4.91$	.010	1.89
	ΔV_Z final	Perturbation timing (unperturbed vs. early vs. mid vs. late)	$F(3,21) = 8.03$	< .001	0.53
		Post-hoc: late > early	$t(7) = 3.41$	.023	1.84
		Post-hoc: late > mid	$t(7) = 6.18$	.003	1.48
		Post-hoc: unperturbed > early	$t(7) = 4.73$	.006	2.07
		Post-hoc: unperturbed > mid	$t(7) = 2.80$	.039	1.63
UCM Wide Targets	ΔV_Z beginning	Perturbation timing (unperturbed vs. early vs. mid vs. late)	$F(3,21) = 2.52$	.086	
	ΔV_Z middle	Perturbation timing (unperturbed vs. early vs. mid vs. late)	$F(3,21) = 2.66$	.074	
	ΔV_Z final	Perturbation timing (unperturbed vs. early vs. mid vs. late)	$F(3,21) = 0.60$	.623	
UCM Perturbed	ΔV_Z beginning	Target type (narrow vs. wide) x perturbation timing (early vs. mid vs. late)	$F(2,14) = 0.78$	.477	
		Main effect: Target type (narrow > wide)	$F(1,7) = 29.23$	.001	0.81
		Main effect: Perturbation timing	$F(2,14) = 0.45$	.647	
	ΔV_Z middle	Target type (narrow vs. wide) x perturbation timing (early vs. mid vs. late)	$F(2,14) = 3.96$	.043	0.36
		Post-hoc narrow: mid > early	$t(7) = 3.90$	.009	1.37

Analysis	Dependent Variable	Factor(s) with Levels	Statistic	*p*	Effect size
		Post-hoc narrow: late > early	$t(7) = 4.81$	.005	1.89
		Post-hoc late: narrow > wide	$t(7) = 6.72$	< .001	1.19
		Main effect: Targe type	$F(1,7) = 1.45$	.267	
		Main effect: Perturbation timing	$F(2,14) = 3.96$	< .001	0.71
		Post-hoc: mid > early	$t(7) = 5.28$	.003	1.87
		Post-hoc: late > early	$t(7) = 3.94$	.008	1.39
	ΔV_Z late	Target type (narrow vs. wide) x perturbation timing (early vs. mid vs. late)	$F(2,14) = 2.48$	.120	
		Main effect: Target type	$F(1,7) = 0.71$	.428	
		Main effect: Perturbation timing	$F(2,14) = 6.29$	.011	0.47
		Post-hoc: late > early	$t(7) = 3.07$	.027	1.09
		Post-hoc: late > mid	$t(7) = 3.10$	.027	1.10
OFC Unperturbed	Endpoint Variability	Target type (wide > narrow)	$t(7) = 5.41$	.001	1.91
OFC Perturbed	Endpoint Variability	Target type (narrow vs. wide) x perturbation timing (early vs. mid vs. late)[a]	$F(1.06,7.43) = 7.43$	.198	
		Main effect: Target type (narrow > wide)	$F(1,7) = 6.06$	.043	0.46
		Main effect: Perturbation timing	$F(2,14) = 1.00$	.392	
OFC Unperturbed	Maximum velocity	Target type	$t(7) = 0.009$	.993	
OFC Perturbed	Maximum velocity	Target type (narrow vs. wide) x perturbation timing (early vs. mid vs. late)	$F(2,14) = 3.68$	.052	
		Main effect: Target type (narrow > wide)	$F(1,7) = 113.82$	< .001	0.94
		Main effect: Perturbation timing	$F(2,14) = 52.94$	< .001	0.88
		Post-hoc: early > mid	$t(7) = 3.27$	.014	1.16
		Post-hoc: early > late	$t(7) = 10.9$	< .001	3.76
		Post-hoc: mid > late	$t(7) = 7.19$	< .001	2.54

Note. Statistic refers to the F-statistic for ANOVA results, and t-statistic for t-test results. Effect size is partial eta-squared ($\eta p2$) for ANOVA results, and Cohen's d for t-test results. Only significant post-hoc tests (i.e., adjusted $p < .05$) are reported, and their p-values are adjusted using FDR.

The sphericity assumption of this repeated-measures ANOVA was violated, so the outcomes of the test were corrected using the Greenhouse-Geisser correction.